Hydrolysis of Thionopeptides by the Aminopeptidase from *Aeromonas proteolytica*: Insight into Substrate Binding†

David L. Bienvenue, Danuta Gilner, and Richard C. Holz*

Department of Chemistry and Biochemistry, Utah State University, Logan, Utah 84322-0300

Received September 4, 2001; Revised Manuscript Received January 17, 2002

ABSTRACT: A series of L-leucine aniline analogues were synthesized that contained either a carbonyl or thiocarbonyl as a part of the amide bond. Additionally, the *para*-position on the phenyl ring of several substrates was altered with various electron-withdrawing or donating groups. The kinetic constants K_m and k_{cat} were determined for the hydrolysis of each of these compounds in the presence of the aminopeptidase from *Aeromonas proteolytica* (AAP) containing either Zn(II) or Cd(II). The dizinc(II) form of AAP ([ZnZn(AAP)]) was able to cleave both carbonyl and thiocarbonyl containing peptide substrates with similar efficiency. However, the dicadmium(II) form of AAP ([CdCd(AAP)]) was unable to cleave any of the carbonyl-containing compounds tested but was able to cleave the thionopeptide substrates. This is consistent with the borderline hard/soft nature of Zn(II) vs Cd(II). The trends observed in the K_m values suggest that the oxygen atom of the amide bond directly interacts with the dinuclear active site of AAP. Heterodimetallic forms of AAP that contained one atom of Zn(II) and one of Cd(II) (i.e., [CdZn(AAP)] and [ZnCd(AAP)]) were also prepared. The K_m values for the thionopeptides substrates are the smallest when Cd(II) is in the first metal binding site, suggesting that substrate binds to the first metal binding site. 1-Phenyl-2-thiourea (PTU) and urea (PU) were also examined to determine the differences between thionopeptide and peptide binding to AAP. PTU and PU were found to be competitive inhibitors of AAP with inhibition constants of 0.24 and 4.6 mM, respectively. The electronic absorption and EPR spectra of [CoCo(AAP)], [CoZn(AAP)], and [ZnCo(AAP)] were recorded in the absence and presence of both PU and PTU. Spectral changes were observed for PTU binding to [CoCo(AAP)] and [CoZn(AAP)] but not for [ZnCo(AAP)], while no spectral changes were observed for any of the Co(II)-substituted forms of AAP upon the addition of PU. These data indicate that carbonyl binding occurs only at the first metal binding site. In light of the data presented herein, the substrate binding step in the proposed mechanism of AAP catalyzed peptide hydrolysis can be further refined.

Hydrolases that contain dinuclear metallo-active sites catalyze the degradation of many of the ubiquitous biomolecules in living organisms such as nucleic acids, phospholipids, and polypeptides (*1*−*4*). They are therefore key-players in carcinogenesis, tissue repair, and protein degradation processes. In addition, dinuclear metallohydrolases are involved in the degradation of agricultural neurotoxins, urea, β-lactam containing antibiotics, and several phosphorus(V) materials used in chemical weaponry (*5*−*7*). Despite their ubiquity and the considerable structural information available, until recently, little has been known about how these structural motifs relate to function (*8*). The importance of understanding the mechanism of action of dinuclear hydrolytic enzymes is underscored by the recent observations that an eukaryotic dinuclear metallo-aminopeptidase is the target for the antitumor drugs ovalicin and fumagillin (*9, 10*). In addition, the naturally occurring peptide analogue inhibitor, bestatin, was recently shown to significantly decrease HIV infection in males by inhibiting aminopeptidase activity (*11*). Thus, the inhibition of aminopeptidase activity in viruses and at malignant tumors is critically important in preventing the growth and proliferation of these types of cells and, for this reason, have become the subject of intense efforts in inhibitor design.

The aminopeptidase from *Aeromonas proteolytica* (AAP)[1] possesses ideal properties for the study of hydrolysis reactions catalyzed by two metal ions (*12*). AAP is a small, monomeric enzyme (32 kDa) that contains two g-atoms of zinc per mole of polypeptide, and is thermostable for several hours at 70 °C. AAP has been crystallographically characterized and possesses a (μ-aqua)(μ-carboxylato)dizinc(II) core with a terminal carboxylate and histidine residue coordinated to each metal ion (*13*). Substitution of the two g-atoms of Zn(II) with Co(II), Cu(II), or Ni(II) provides enzymes that are hyperactive by 7.7, 6.5, and 25 times, respectively, toward

†This work was supported by the National Science Foundation (CHE-9816487; RCH).

* Address correspondence to: Richard C. Holz, Department of Chemistry and Biochemistry, Utah State University, Logan, UT 84322-0300, Phone (435) 797-2609, Fax: (435) 797-3390, Internet: rholz@cc.usu.edu.

[1] Abbreviations: HEPES ([4-(2-hydroxyethyl)-1-piperazineethanesulfonic acid]); TLA (thionoleucine-*S*-anilide); LA (L-leucine anilide); LAD (L-leucine anisidide); TLAD (thionoleucine-*S*-anisidide); L-*p*NA (L-leucine-*p*-nitroaniline); LAMC (L-leucine-7-amido-4-methylcoumarin hydrochloride); PU (phenylurea); PTU (1-phenyl-2-thiourea) AAP (aminopeptidase from *Aeromonas proteolytica*); blLAP (bovine lens leucine aminopeptidase); EPR (electron paramagnetic resonance).

10.1021/bi011752o CCC: $22.00
Published on Web 02/23/2002

certain substrates (*14*−*16*). Moreover, Bennett and Holz recently demonstrated that metal binding to AAP occurs in a sequential fashion (*17*), highlighting the potential for heterodimetallic centers. Heterodimetallic sites allow the function of each metal binding site to be studied through independent labeling with spectroscopically active and silent metal ions, respectively. Upon the basis of the structural, kinetic, and spectroscopic studies reported to date, a detailed reaction mechanism was recently proposed for AAP (*8*). However, despite the wealth of mechanistic data available for AAP, little is known about how the structural motif of the resting enzyme relates to the substrate-binding step in peptide hydrolysis.

In an effort to further define the substrate-binding step in the catalytic mechanism of peptide hydrolysis catalyzed by two metal ions, we report herein the effect of replacing the carbonyl oxygen of various substrate analogues with sulfur on the rates of hydrolysis catalyzed by both the Zn(II)- and Cd(II)-substituted AAP enzymes. It has previously been shown that the leucine aminopeptidase from bovine lens is inhibited by thionoamide derivatives of L-leucine (*18*), and the peptide deformylase from *Escherichia coli* lacks the ability to cleave thionopeptide derivatives (*19*). However, carboxypeptidase A has the ability to cleave sulfur derivatives of its common substrates (*20*), and urease can react with thiourea (*21*). These enzymes differ in their ligand type and metal ion coordination geometry, both of which are directly related to their ability to bind a carbonyl oxygen atom and, thus, cleave peptides. In addition, two small peptide derivatives, phenylurea and phenylthiourea, were examined to define the differences in carbonyl vs thiocarbonyl binding to AAP. Analysis of the kinetic and spectroscopic data for carbonyl and thionocarbonyl binding to the dinuclear active site of AAP has provided additional information on the substrate binding step in peptide hydrolysis.

MATERIALS AND METHODS

Materials. *N*-t-Boc-L-leucine monohydrate was purchased from Sigma, aniline, *p*-methoxyaniline, 2.0 M solution of hydrochloric acid in diethyl ether and silica gel (200−400 mesh, 60 Å) were purchased from Aldrich, trifluoroacetic acid was from EM Science, and *N*,*N*′-dicyclohexylcarbodiimide and Lawesson's reagent (2,4-bis(4-methoxyphenyl)-1,3-dithia-2,4-diphosphethane-2,4-disulfide) were purchased from Acros. All solvents were purchased from Fisher, and distilled and dried as needed.

Synthetic Methods. *L-Leucine Anilide Hydrochloride (LA).* Boc-L-Leu-NHPh HCl was synthesized from Boc-L-leucine and aniline using the coupling reaction with *N*,*N*′-dicyclohexylcarbodiimide (*22*). The product was deprotected using 2.0 M HCl in diethyl ether. NMR (270 MHz, DMSO) δ (ppm): 10.92 (s, 1H), 8.44 (broad s, 3H), 7.66 (d, 2H, *J* 7.9 Hz), 7.34 (t, 2H, *J* 7.9 Hz), 7.10 (t, 1H, *J* 7.4 Hz), 4.04 (m, 1H), 1.69 (m, 3H), 0.92 (m, 6H). Elemental analysis calculated for $C_{12}H_{19}N_2OCl$ 242.75: required C 59.38%, H 7.89%, N 11.54%; found C 59.49%. H 7.83%, N 11.51%. mp 240−241 °C.

Thionoleucine-S-anilide Hydrochloride (TLA). Thionoleucine *S*-anilide hydrochloride was synthesized using the method described by Beattie et al. (*18*). NMR (270 MHz, DMSO) δ (ppm) 12.73 (s, 1H), 8.43 (s, 3H), 7.89 (d, 2H, *J* 8.2 Hz), 7.44 (t, 2H, *J* 7.9 Hz), 7.29 (t, 1H, *J* 7.3 Hz), 4.57 (m, 1H), 1.57−1.85 (m, 3H), 0.96 (d, 3H, *J* 14.8 Hz), 0.94 (d, 3H, *J* 14.8 Hz). Elemental analysis calculated for $C_{12}H_{19}N_2SCl$ 258.82: required C 55.69%, H 7.40, N 10.82%, S 12.39%; found C 55.54%; H 7.30%, N 10.82%; S 12.23%. mp 226−227 °C.

L-Leucine-p-anisidide Hydrochloride (LAD). Boc-L-leucine-*p*-anisidide was synthesized using the method described by Taylor et al. (*23*). L-Leucine-*p*-anisidide hydrochloride was obtained by deprotection of Boc-L-leucine-*p*-anisidide with 2.0 M HCl in diethyl ether. NMR (270 MHz, DMSO) δ (ppm) 10.79 (s, 1H), 8.42 (broad s, 3H), 7.56 (d, 2H, *J* 9.4 Hz), 6.91 (d, 2H, *J* 9.4 Hz), 3.99 (m, 1H), 3.72 (s, 3H), 1.66 (m, 3H), 0.92 (m, 6H). Elemental analysis calculated for $C_{13}H_{21}O_2N_2Cl$ 272.78: required C 57.24%, H 7.76%, N 10.27%; found C 57.23%, H 7.84%, N 10.23%. mp 189−190 °C.

Thionoleucine-S-p-anisidide Hydrochloride (TLAD). Thionoleucine S-*p*-anisidide hydrochloride was synthesized using the method described by Beattie et al. (*18*). NMR (270 MHz, DMSO) δ (ppm) 12.61 (s, 1H), 8.43 (s, 3H), 7.80 (d, 2H, *J* 8.9 Hz), 6.98 (d, 2H, *J* 8.9 Hz), 4.52 (m, 1H), 3.77 (s, 3H), 1.50−1.89 (m, 3H), 0.95 (d, 3H, *J* 15.2 Hz), 0.93 (d, 3H, *J* 15.2 Hz). Elemental analysis calculated for $C_{13}H_{21}N_2OSCl$ 288.84: required C 54.06%, H 7.33%, N 9.70%, S 11.10%; found C 53.83%, H 7.30%, N 9.63%, S 10.97%. mp 208−209 °C.

Purification of AAP. The aminopeptidase from *Aeromonas proteolytica* was purified from a stock culture kindly provided by Professor Céline Schalk. Cultures were grown according to the previously published procedure (*24*) with minor modifications to the growth media (*25*). Purified enzyme was stored at −80 °C until needed.

Spectrophotometric Assay of AAP. AAP activity was measured by the method of Prescott and Wilkes (*12*) as modified by Baker et al. (*26*). In this assay, the hydrolysis of 0.5 mM L-leucine-*p*-nitroanilide (L-*p*NA) (10 mM Tricine, pH 8.0 containing 0.1 mM $ZnSO_4$) was measured spectrophotometrically at 25 °C by monitoring the formation of *p*-nitroaniline. The extent of hydrolysis was calculated by monitoring the increase in absorbance at 405 nm (ϵ_{405} value of *p*-nitroaniline of 10 800 $M^{-1}cm^{-1}$) (*27*). One unit was defined as the amount of enzyme that releases 1 μmol of *p*-nitroaniline at 25 °C in 60 s. The specific activity of purified AAP was typically found to be 120 units per mg of enzyme. This value is identical to that reported by Prescott and Wilkes (*12*). All spectrophotometric assays were performed on a Shimadzu UV-3101PC spectrophotometer equipped with a constant-temperature cell-holder. Enzyme concentrations were determined from the absorbance at 278 nm with the value $\epsilon_{278} = 41\,800\ M^{-1}\ cm^{-1}$ (*28*).

Kinetics Studies of Amide and Thionoamide Hydrolysis. The rate of hydrolysis of L-leucine-anilide (LA), thionoleucine-*S*-anilide (TLA), L-leucine-*p*-anisidide (LAD), and thionoleucine-*p*-anisidide (TLAD) was determined by measuring the decrease in absorbance of the amide or thionoamide bond (295 nm for TLA, TLAD, 240 nm for LA, LAD) for 120 s. Aniline and *p*-anisidine, both potential hydrolysis products, absorb light at the wavelengths chosen to monitor rates of reaction, while L-leucine was not found to absorb a significant amount of light at either 240 or 295 nm. The extinction coefficient of each substrate and potential product

was determined, and initial velocities were calculated using the difference in extinction coefficient, $\Delta\epsilon$, between each substrate and its respective product. The rates of AAP-catalyzed hydrolysis of LA, TLAD, TLA, L-*p*NA, and LAD were determined at several substrate concentrations and different metal-containing forms of AAP. The decrease in absorbance resulting from the cleavage of all the substrate analogues used was linear over the course of 120 s indicating the steady-state had been achieved. Control experiments in which assays were performed in the presence or absence of excess (~1 mM) metal yielded identical results, indicating that substrate was not interacting with free metal in solution. The kinetic parameters K_m and k_{cat} were determined by fitting the experimental data to the Michaelis−Menten equation via an iterative process. Each measurement was made in triplicate, and the error values represent the standard deviation for each kinetic constant.

Inhibition Studies. All kinetic experiments were performed in 10 mM Tricine buffer, pH 8.0, at 25 °C. The inhibition constant (K_i) for phenylurea and 1-phenyl-2-thiourea was determined spectrophotometrically by measuring the initial velocity of L-leucine-7-amido-4-methylcoumarin (LAMC) hydrolysis at 360 nm (ϵ_{360} = 7800 $M^{-1}cm^{-1}$) at varying LAMC and inhibitor concentrations. LAMC was used instead of the typical leucine aminopeptidase substrate, L-*p*NA, since previous research showed that interactions between L-*p*NA and thionoamides could occur (*18*). Each experiment was performed in triplicate and fit to the Michaelis−Menten equation for competitive inhibition to determine the inhibition constants for phenylurea and 1-phenyl-2-thiourea.

Preparation of Cadmium and Cobalt Derivatives of AAP. Apo-AAP was prepared by incubating the purified enzyme with 10 mM EDTA for 3−4 days, then extensively dialyzing against 50 mM chelexed Hepes buffer, pH 7.5. The presence of residual zinc was determined via the measurement of L-*p*NA hydrolysis by apo-enzyme. Apo-AAP typically has less than 5% of the activity of the fully loaded-Zn(II) form of the enzyme. Heterogeneous derivatives of AAP in which two different transition metal were present in the active site were prepared by adding one equivalent of either Zn(II), Cd(II), or Co(II) to apo-enzyme, followed by rapid mixing. After a 20-min incubation period, a second equivalent of metal was added. AAP samples containing Co(II) were prepared anaerobically inside a glovebox using degassed buffers. The addition of excess Zn(II) or Cd(II) did not alter the rates of hydrolysis observed. The metals used in these experiments were of the highest purity obtainable (≥99.999% $CoCl_2$, and $CdCl_2$, Strem Chemicals; 99.999% $ZnCl_2$, Aldrich).

Spectroscopic Measurements. All spectrophotometric experiments were performed on a Hewlett-Packard 8453 spectrophotometer inside an anaerobic chamber. Samples were placed in a 200 μL, 1-cm path-length microcuvette (QS, Hellma). The absorption spectrum of apo AAP was subtracted from the spectra of all metal-substituted samples using IgorPro (Wavemetrics, Inc.). Enzyme concentrations were typically 1 mM and when PU or PTU was added they were at saturating concentrations (~6 mM). Low-temperature, dual-mode EPR spectroscopy was performed on a Bruker ESP-300E spectrometer equipped with an ER 4116 DM dual mode X-band cavity and Oxford Instruments ESR-900 helium flow cryostat. Perpendicular mode spectra were recorded at a frequency of about 9.63 GHz and frequency modulation amplitude of 100 kHz. Exact microwave frequencies were recorded for each spectrum to ensure precise g-alignment.

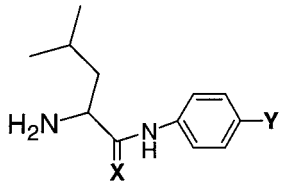

LA	X = O	Y = H
LAD	X = O	Y = OCH_3
TLA	X = S	Y = H
TLAD	X = S	Y = OCH_3

FIGURE 1: Chemicals used as potential substrates for AAP-catalyzed hydrolysis, where X represents either a sulfur or oxygen atom, and Y represents the *para*-substituent on the phenyl ring.

RESULTS

Kinetic Studies on Peptide and Thionopeptide Hydrolysis. Thionoleucine-*S*-anilide (TLA) and thionoleucine-*p*-anisidide (TLAD) were examined as substrates for AAP (Figure 1). The decrease in absorbance resulting from cleavage of the thionoamide bond was observed, and was linear over 120 s for both TLAD and TLA. Significant differences in the k_{cat} and K_m values were observed for the various thiocarbonyl and carbonyl-containing substrates (Table 1). The dicadmium(II) form of AAP, [CdCd(AAP)], exhibited no detectable activity with any of the oxygen-containing compounds even after increasing the enzyme concentration 5-fold to 50 μM and the amount of time 10-fold, to 10 min. On the other hand, [CdCd(AAP)] and [ZnZn(AAP)] exhibit very similar rates of cleavage for the two thionoamide substrates. When the K_m values are compared, it is apparent that [ZnZn(AAP)] binds TLA and TLAD more tightly than their exact oxygen analogues since there is a ~30% decrease in magnitude of K_m. Comparison of the K_m values for [CdCd(AAP)] and [ZnZn(AAP)] indicates that Cd(II)-substituted AAP binds the thiocarbonyl-containing substrates slightly tighter than Zn(II) AAP (TLA $K_m = 8.0 \pm 4.0$ μM versus $K_m = 10.0 \pm 0.5$ μM, TLAD $K_m = 4.0 \pm 1.0$ μM versus $K_m = 7.0 \pm 0.4$ μM).

To determine if the carbonyl or thiocarbonyl group of the substrate interacts with one or both metal binding sites, heterodimetallic samples of AAP were prepared that contained both Cd(II) and Zn(II) in the active site. When Cd(II) was placed in the first metal binding site ([CdZn(AAP)]), little change was observed in the rates of cleavage of LA (L-leucine anilide) (15.1 ± 0.8 s^{-1}) and LAD (L-leucine anisidide) (9.3 ± 0.6 s^{-1}) when compared to [ZnZn(AAP)] (16.0 ± 1.3 and 9.5 ± 0.8 s^{-1}), while a decrease in k_{cat} occurs for both TLA and TLAD from ~11 to ~7.5 s^{-1}. Placing Cd(II) in the second site of AAP ([ZnCd(AAP)]) causes a significant decrease in k_{cat} for both oxygen derivatives. The k_{cat} for LA drops from 16.0 ± 1.3 to 6.3 ± 0.4 s^{-1}, while the k_{cat} for LAD decreases from 9.5 ± 0.8 to 3.8 ± 0.1 s^{-1}. The rates of hydrolysis for TLA and TLAD catalyzed by [ZnCd(AAP)] increase substantially as compared to [ZnZn(AAP)] for TLA (11.5 ± 0.4 to 23.3 ± 0.5 s^{-1}), but remain relatively unchanged for TLAD (11.1 ± 0.3 to 12.2 ± 0.2 s^{-1}).

Table 1: Kinetic Parameters for Cd(II) Homo- and Heterodiatomic Substituted AAP with Thio and Carbonyl Containing Substrates

	L-*p*-NA		LTA		TLAD		LA		LAD	
enz	k_{cat} (s^{-1})	K_m (mM)	k_{cat} ($_s^{-1}$)	K_m (mM)	k_{cat} (s^{-1})	K_m (mM)	k_{cat} (s^{-1})	K_m (mM)	k_{cat} (s^{-1})	K_m (mM)
CdCd	ND	ND	10.6 ± 0.5	8.0 ± 4.0	7.9 ± 0.4	4.0 ± 1.0	ND	ND	ND	ND
ZnZn	60 ± 0.3	15.0 ± 4.0	11.5 ± 0.4	10.0 ± 0.5	11.1 ± 0.3	7.0 ± 0.4	16.0 ± 1.3	78.0 ± 15.0	9.5 ± 0.8	50.0 ± 11.0
CdZn	3.0 ± 0.4	4.6 ± 1	7.7 ± 0.4	4.0 ± 1.0	7.5 ± 0.4	4.0 ± 1.0	15.1 ± 0.8	61.0 ± 4.0	9.3 ± 0.6	34.0 ± 4.0
ZnCd	5.3 ± 0.6	7.8 ± 0.3	23.3 ± 0.5	11.0 ± 2.0	12.2 ± 0.2	5.0 ± 0.2	6.3 ± 0.4	45.0 ± 6.0	3.8 ± 0.1	32.0 ± 4.0

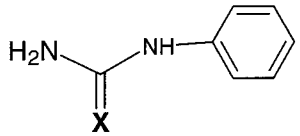

Phenyl urea X = O
Phenyl thiourea X = S

FIGURE 2: Structures of PU (X = oxygen) and PTU (X = sulfur).

The effect of different substituents at the *para*-position of the phenyl ring of the substrate leaving group on the observed activity of AAP was also examined. The native form of AAP, [ZnZn(AAP)], appears to have the highest catalytic activity with L-*p*NA (60 ± 0.3 s^{-1}), similar to that previously reported for AAP (67 s^{-1}) (*12*). The *p*-methoxy moiety on the TLAD and LAD leaving groups appear to decrease the rates of hydrolysis by all of the metal-substituted forms of AAP. The k_{cat} values of [ZnCd(AAP)] for TLAD (12.2 ± 0.2) and LAD (3.8 ± 0.1) are approximately half of those obtained with their exact anilide derivatives. There also appears to be an increase in the affinity of substrate since all the derivatives of AAP, with the exception of [CdZn(AAP)] when binding the thiocarbonyl compounds, exhibit a decrease in K_m. When -H is the *para*-substituent, the values of k_{cat} are intermediate between those obtained when $-NO_2$ and $-OCH_3$ are in the *para*-position.

Inhibition of AAP by Phenylurea and 1-Phenyl-2-thiourea. Phenylurea (PU) and 1-phenyl-2-thiourea (PTU) have backbone structures that are similar to TLA and LA (Figure 2). Incubation of a 1 mM sample of either PU or PTU with AAP while monitoring the absorbance at 215 nm for 30 min revealed that AAP does not cleave either compound. Inhibition of AAP activity by PTU and PU was examined at several different concentrations of L-leucine-7-amidomethylcoumarin (LAMC). LAMC was used instead of the typical leucine aminopeptidase substrate, L-*p*NA, since previous research showed that interactions between L-*p*NA and thionoamides could occur (*18*). In the absence of inhibitor, the K_m value of AAP for LAMC was determined to be 40 μM with a k_{cat} value of 0.07 s^{-1}. Replotting the experimental data obtained for both PTU and PU in the Lineweaver−Burke format resulted in a series of intersecting lines consistent with the expected pattern for a competitive inhibitor. These data were fit to the Michaelis−Menten equation for competitive inhibition, and the inhibition constants were determined to be 4.6 mM for PU and 0.24 mM for PTU.

Absorption Spectra of PU and PTU Bound to Co(II)-Substituted AAP. Electronic absorption spectra were recorded for [CoCo(AAP)] (Figure 3) and found to be identical to the spectra previously recorded (*29*, *30*). The absorption spectrum of apo-AAP was subtracted from all spectra. [CoCo(AAP)] exhibits an absorption maxima at 525 nm with a molar absorptivity of ~80 M^{-1} cm^{-1}. Upon the addition

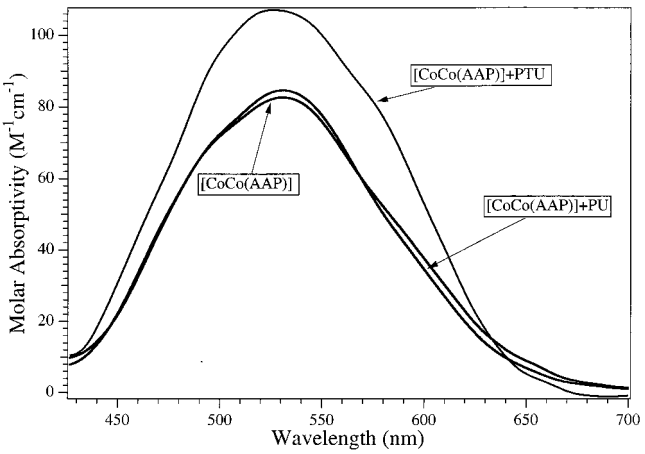

FIGURE 3: Electronic absorption spectra of 1 mM [CoCo(AAP)] in 50 mM HEPES buffer at pH 7.5 recorded in the presence and absence of PTU and PU. The electronic absorption spectrum of apo-enzyme was subtracted in each case.

of six equivalents of PTU, an increase in the molar absorptivity was observed from ~80 to ~105 M^{-1} cm^{-1} (Figure 3). This change is concomitant with an overall broadening of the spectrum, although the position of the major absorption band did not change. The absorption spectrum of [CoCo(AAP)] was also recorded in the presence of PU (Figure 3). The molar absorptivity and the λ_{max} values do not change, indicating that phenyl urea binds very weakly or does not interact with the dicobalt(II) center of AAP. Electronic absorption spectra of [CoCo(AAP)] in the presence of both PU and PTU were also recorded in the 250 to 400 nm range; however, no absorption band was observed between 300 and 450 nm characteristic of an S → Co(II) ligand-to-metal charge-transfer (LMCT) band.

The absorption spectra of [CoZn(AAP)] and [ZnCo(AAP)] were recorded before and after the addition of PU and PTU (Figure 4). The molar absorptivity of [CoCo(AAP)] is essentially the sum of the molar absorptivities of [CoZn-(AAP)] and [ZnCo(AAP)], indicating that the two metal ions in these heterogeneous forms must maintain similar geometries in the dicobalt-substituted form of AAP. There is no change upon the addition of PU to the absorption spectrum of either [CoZn(AAP)] or [ZnCo(AAP)]. However, when PTU is added to [CoZn(AAP)], the same increase noted in the spectrum of dicobalt AAP after the addition of PTU is observed. The molar absorptivity of [CoZn(AAP)] increases from ~47 to ~69 M^{-1} cm^{-1} without any apparent shift in the position of the maximum absorbance. On the other hand, the addition of PTU to [ZnCo(AAP)] does not cause any significant change in the absorption spectra.

The EPR spectra of [CoCo(AAP)], [CoZn(AAP)], and [ZnCo(AAP)] were recorded in both the absence and presence of PU and PTU (Figures 5 and 6). Examination of the spectrum of [CoCo(AAP)] and [CoZn(AAP)] upon the

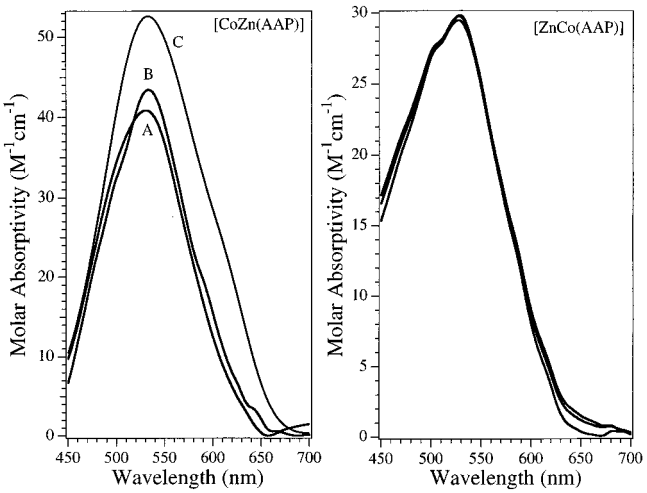

FIGURE 4: Electronic absorption spectra of 1 mM [CoZn(AAP)] (left panel) and [ZnCo(AAP)] (right panel) in 50 mM HEPES buffer at pH 7.5 recorded in absence (A) and presence of PU (B) and PTU (C). The electronic absorption spectrum of apo enzyme was subtracted in each case.

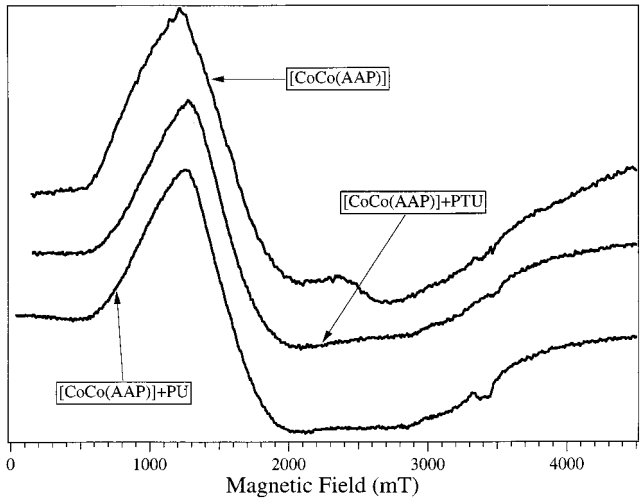

FIGURE 5: EPR spectra of 1 mM [CoCo(AAP)] in 50 mM HEPES buffer at pH 7.5 recorded in the presence and absence of PTU and PU. All spectra were recorded using 100 kHz modulation frequency, 1.26 mT modulation amplitude, 3.l2 mT s^{-1} field sweep rate, and 164 ms time constant.

addition of PTU suggests that the electronic environment of the two cobalt ions are perturbed, but not markedly when inhibitor binds (Figures 5 and 6). On the other hand, the addition of PTU to [ZnCo(AAP)] does not cause any detectable change in the EPR spectrum (Figure 6), suggesting that PTU does not interact with the Co(II) ion in the second metal binding site. Examination of [CoCo(AAP)] with or without either inhibitor at higher temperatures (40 K) and powers (50 mW) does not result in any other visible differences in the spectra. Upon the addition of PU to [CoCo-(AAP)], [CoZn(AAP)], and [ZnCo(AAP)], no observable change was detected in any of the EPR spectra recorded.

DISCUSSION

Previous crystal structures of AAP with inhibitors bound to the active site suggest that the carbonyl oxygen atom of the N-terminal amino acid residue binds to the first metal binding site (Zn_1) (*8*, *31*, *32*). It was proposed that Zn_1 was responsible for polarizing the carbonyl bond as well as

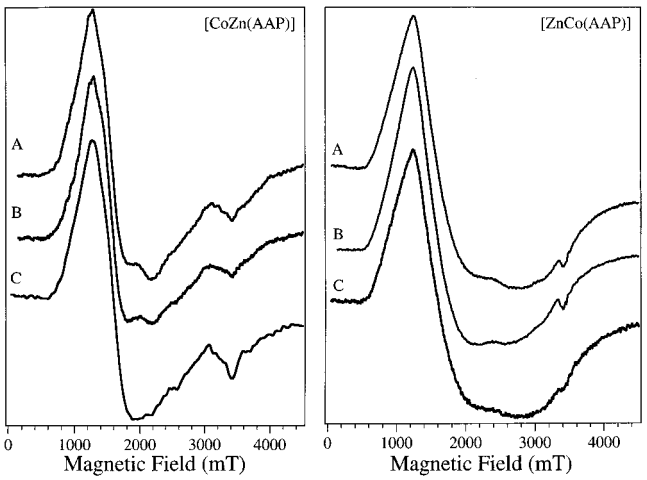

FIGURE 6: EPR spectra of [CoZn(AAP)] (left panel) and [ZnCo-(AAP)] (right panel) in 50 mM HEPES buffer at pH 7.5 recorded in the absence (A) and presence of PU (B) and PTU (C). All spectra were recorded using 100 kHz modulation frequency, 1.26 mT modulation amplitude, 3.l2 mT s^{-1} field sweep rate, and 164 ms time constant.

delivering the hydroxide nucleophile, thus explaining why AAP has approximately 80% of its native activity with just the first metal binding site occupied (*8*). On the other hand, the N-terminal amine acts as a ligand to the second metal center (Zn_2), which was hypothesized to assist in binding and positioning the substrate for nucleophilic attack. Despite the structural evidence from transition-state analogue inhibitors for the possible roles of both Zn(II) ions in substrate binding, little is actually known about how substrate binds to AAP. Therefore, the AAP-catalyzed hydrolysis of peptides was examined for a series of thionocarbonyl and their exact carbonyl substrate analogues. It has previously been shown that the leucine aminopeptidase from bovine lens (blLAP) is inhibited by thionoleucine-*S*-anilide (TLA) with an inhibition constant of 190 μM (*18*). Similarly, the peptide deformylase from *E. coli* lacks the ability to cleave thionopeptide derivatives (*19*). However, carboxypeptidase A (CPA) has the ability to cleave thionocarbonyl derivatives of its common substrates (*21*). Interestingly, when the native Zn(II) ion in CPA was replaced with other transition metal ions, (i.e., Cd(II)) changes in both k_{cat} and K_m were observed for both the oxygen- and sulfur-containing compounds (*33*). On the basis of these data, it was proposed that CPA utilizes the Zn(II) ion to bind the substrate carbonyl oxygen atom and polarize the C−O bond. Since each of these enzymes have different active site ligands, coordination numbers, and geometries, their ability to cleave peptides and/or thionopeptides is directly related to the ability of the active site metal ion to bind and polarize the backbone carbonyl.

The dizinc(II) form of AAP was observed to have the ability to cleave both thionocarbonyl and carbonyl containing substrates. These data are consistent with the active site Zn-(II) ions having the ability to bind both hard and soft ligands. However, Cd(II)-substituted AAP cannot cleave carbonyl containing substrates such as LA, LAD, or L-*p*NA. Similarly, the Cd(II)-substituted form of CPA was inactive against carbobenzyloxyglycylglycyl-L-phenylalanine, a well-characterized substrate of the native Zn(II) form of CPA (*20*). The lack of observed hydrolysis of carbonyl containing substrates for Cd(II)-substituted enzymes is likely the result

of insufficient polarization of the carbonyl bond to permit nucleophilic attack by an hydroxide ion. For AAP, both [CdCd(AAP)] and [ZnZn(AAP)] have very similar K_m and k_{cat} values for thionopeptide substrates, indicating that Cd(II) does not confer any significant advantage to AAP for binding and hydrolyzing thionoamide substrates. When the K_m values of dizinc(II) AAP are compared for the different substrates studied, it is clear that the thionoamide compounds bind more tightly than their carbonyl analogues. These data suggest that substrate binding to AAP involves direct interaction between the oxygen atom of the amide bond and the metal ions bound to the active site, since the only structural difference is the exchange of sulfur for oxygen. If the divalent metal ions in the active site of AAP served only to deliver an hydroxide ion, it would be expected that [CdCd(AAP)] would be able to cleave both amide and thionoamide substrates. Similarly, the exchange of oxygen for sulfur would not be expected to alter the K_m values if the binding of these substrates to AAP did not involve the metal center.

The proposed mechanism for AAP designates specific roles for each of the metal ions in the catalytic process (*29*). When Cd(II) is placed in the first metal binding site of AAP, [CdZn(AAP)], little change is observed in the rates of cleavage of LA and LAD as compared with [ZnZn(AAP)], while a decrease in k_{cat} occurs for both TLA and TLAD. Placing Cd(II) in the second metal binding site of AAP causes a significant decrease in k_{cat} for both of the oxygen derivatives, while the rates of hydrolysis for TLA and TLAD increase substantially. The rate-limiting step of AAP-catalyzed hydrolysis of peptides has previously been shown to be the collapse of the tetrahedral transition state (*25*). Therefore, the rate of this step should be reflected in the magnitude of k_{cat}. If the transition state was only stabilized by Zn_1, then the values of k_{cat} for [ZnCd(AAP)] and [ZnZn(AAP)] should be identical. Similarly, the rates of hydrolysis for the thionoamide compounds obtained with [CdCd(AAP)] would be the same as [CdZn(AAP)]. However, k_{cat} is affected when the divalent metal ion in the second site of [CdCd(AAP)] and [ZnZn(AAP)] is replaced to form a heterodimetallic active site. These data suggest that both metal ions are involved in stabilizing the transition-state of the reaction, consistent with the proposed mechanism of AAP (*29*). There also appears to be a synergistic effect when two different metal ions are bound in the active site of AAP, since the fastest rates of hydrolysis are obtained with [ZnCd(AAP)]. Similar effects have been observed for [CuZn(AAP)], [NiZn(AAP)], and [CoZn(AAP)] (*15*). All three of these heterodimetallic samples were shown to have higher catalytic efficiency than their homodimetallic counterparts.

While the data presented thus far suggest that both metal centers affect the values of k_{cat}, the trends observed in K_m imply that only Zn_1 is involved in binding substrate. The K_m values for thionoamides are the lowest when Cd(II) is in the first metal binding site of AAP. Conversely, the largest K_m values for the amide derivatives are obtained when Cd(II) is in the first metal binding site. It has previously been shown that urease, an enzyme containing a dinuclear Ni(II) center, binds urea more tightly than thiourea (*21*). Since Ni(II) is considered a soft acid and sulfur a soft base, the authors suggested that substrate binding does not involve a direct interaction with the dinuclear active site. Because of the preference of Cd(II) for sulfur, the trends in the K_m values observed for AAP suggest that the carbonyl oxygen atom of the substrate interacts with the first metal binding site of AAP. Although Zn(II) is a borderline hard/soft transition metal and should be able to bind either oxygen or sulfur with similar affinity, AAP appears to have a greater affinity for amide compounds when Zn(II) is in the first metal binding site.

In addition to examining the effects of replacing the carbonyl oxygen atom with sulfur, substrate analogues were synthesized that had both electron donating and withdrawing moieties attached to the leaving groups. For example, a *p*-methoxy moiety can act as an electron-donating group and, therefore, should stabilize the amide bond making it less susceptible to cleavage. As expected, the rates of cleavage observed for the AAP catalyzed hydrolysis of the *p*-methoxy containing substrates LAD and TLAD are lower than their structural analogues that only contain a *p*-hydrogen atom. Although the *p*-methoxy group decreases the rate of hydrolysis, the electron-donating properties of this substituent facilitates tighter binding to AAP based on the smaller K_m values observed relative to the compounds containing only a phenyl ring. This is likely because the sulfur or oxygen atoms of the carbonyl group can donate a greater amount of electron density to maintain charge neutrality about the metal ion. A *p*-nitro group functions in the opposite fashion of the *p*-methoxy group in that electron density is drawn away from the amide bond, helping to stabilize the negative charge building up on the nitrogen atom during catalysis. Because *p*-nitroaniline is a better leaving group, high rates of cleavage are observed. The K_m (17 μM) and k_{cat} (60 s^{-1}) values of L-*p*NA for [ZnZn(AAP)] are consistent with the trends observed for LAD and LA (i.e., as the potential leaving group of the substrate improves, so does the rate of catalysis). The other metal-substituted forms of AAP exhibit greater rates of hydrolysis with either the -OCH_3 or -H substituted substrates, implying that there may also be other factors involved such as hydrogen bonding.

Previously, it was shown that thiol-containing compounds are potent inhibitors of AAP (*34*, *35*). For example, L-leucinethiol is a slow-binding competitive inhibitor of AAP with an overall K_i of 7 nM, while the exact alcohol derivative (L-leucinol) is a weak competitive inhibitor, exhibiting a K_i of 17 μM (*34*). Comparison of the inhibition constants of PU and PTU indicate that a similar trend exists for carbonyl vs thionocarbonyl derivatives of the same compound (4 vs 0.24 mM, respectively). The K_i value determined for PTU is substantially larger than values obtained for thiol-inhibitors of AAP, implying that the thionoamide bond does not undergo isomerization to its thiol form upon binding to AAP. When the inhibitory properties of thiol and thionoamide derivatives of the same compound were tested against peptide deformylase, identical trends were observed with the thiol compound having a K_i value at least 200 times less than its exact thionoamide derivative (*19*). Since the only difference between PU and PTU is the exchange of a sulfur atom for an oxygen atom, the differences in K_i must result from the interaction of this portion of the molecule with the dinuclear active site of AAP. Similar results were observed for urease in the presence of urea and thiourea (*21*). It was found that urea binds nearly 30 times more tightly to urease than its thiourea analogue. The fact that urease has a greater affinity for urea was taken to mean that the catalytic mechanism of

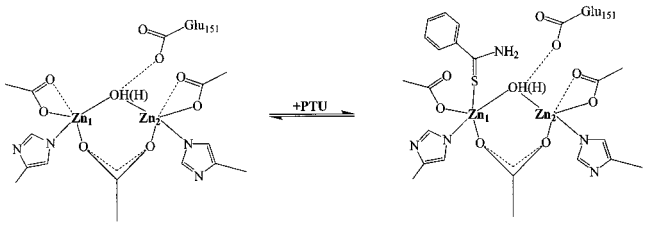

FIGURE 7: Proposed binding mode of PTU to the dinuclear active site of AAP.

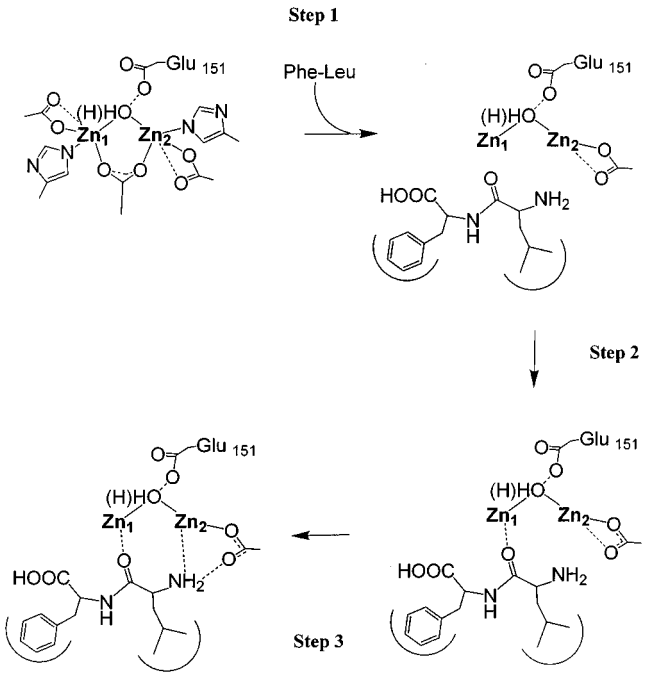

FIGURE 8: Proposed first three steps in the peptide hydrolysis reaction catalyzed by AAP.

urease does not involve direct interaction between the substrate and metal ions. Conversely, the kinetic data obtained for the L-leucine substrates of AAP as well as the inhibition of AAP by PU and PTU suggest that the metal ions in AAP are directly involved in substrate binding.

The ability of AAP to bind metal ions sequentially can be exploited to examine inhibitor binding to each metal binding site independently of one another. The electronic absorption and EPR spectra of [CoCo(AAP)], [CoZn(AAP)], and [ZnCo(AAP)] were recorded in the presence and absence of PU and PTU. The absorption spectra of [CoCo(AAP)] and [CoZn(AAP)] change upon the addition of excess PTU, while the spectrum of [ZnCo(AAP)] is not affected. This implies that PTU binds to the active site of AAP via interaction with the first metal binding site without affecting the environment or geometry about the second metal binding site (Figure 7). On the other hand, the absorption spectra of [CoCo(AAP)], [CoZn(AAP)], and [ZnCo(AAP)] are not affected upon the addition of PU, suggesting that this inhibitor either binds the active site metal ions very weakly or does not interact with the dinuclear active site. Although the EPR spectrum of [CoCo(AAP)] and [CoZn(AAP)] do not change drastically in the presence of PTU, there are some distinct changes in the shape and positions of the g values that suggest that PTU interacts with the Co(II) ions bound to the active site of AAP. The g_1 feature at 5.7 shifts to 5.4, while the feature at 2.9 disappears in the presence of either inhibitor. This is unlike the spectra of other thiolate-inhibitors bound to the active site of AAP in which a sharp feature at $g \approx 6.5$ appears that is typical for a Co(II)-thiol interactions (*34*, *35*). The lack of such a signal upon the addition of PTU to [CoCo(AAP)] and [CoZn(AAP)] suggests that PTU remains in its thiocarbonyl form when bound to AAP and does not form the thiolate to any great extent.

In conclusion, the data presented herein provide insight into the substrate-binding step of the peptide hydrolysis reaction catalyzed by AAP. Previous studies on a series of aliphatic alcohols suggested that the initial step in substrate binding is the interaction of the N-terminal amino acid moiety with the hydrophobic pocket that exists in close proximity to the dinuclear Zn(II) active site of AAP (*25*). On the basis of the kinetic and spectroscopic data reported herein, the second step in catalysis is carbonyl binding to Zn_1 (Figure 8). The kinetic data in this study suggest that this interaction is essential for activating the carbon atom of the amide bond for nucleophilic attack. On the basis of X-ray crystallographic and kinetic data, the third step in catalysis is the interaction of the N-terminal amine with Zn_2 (Figure 8) (*30*, *34*). After nucleophilic attack of the metal-bound hydroxide ion on the scissile carbonyl carbon, a tetrahedral transition state is formed which is stabilized via interaction with both metal centers (*8*).

REFERENCES

1. Dismukes, G. C. (1996) *Chem. Rev. 96*, 2909−2926.
2. Sträter, N., Lipscomb, W. N., Klabunde, T., and Krebs, B. (1996) *Angew. Chem., Int. Ed. Engl. 35*, 2024−2055.
3. Lipscomb, W. N., and Sträter, N. (1996) *Chem. Rev. 96*, 2375−2433.
4. Wilcox, D. E. (1996) *Chem. Rev. 96*, 2435−2458.
5. Chin, J. (1991) *Acc. Chem. Res. 24*, 145−152.
6. Lai, K., Dave, K. I., and Wild, J. R. (1994) *J. Biol. Chem. 269*, 16579−16584.
7. Menger, F. M., Gan, L. H., Johnson, E., and Durst, D. H. (1987) *J. Am. Chem. Soc. 109*, 2800−2803.
8. Stamper, C., Bennett, B., Edwards, T., Holz, R. C., Ringe, D., and Petsko, G. (2001) *Biochemistry 40*, 7035−7046.
9. Sin, N., Meng, L., Wang, M. Q., Wen, J. J., Bornmann, W. G., and Crews, C. M. (1997) *Proc. Natl. Acad. Sci. U.S.A. 94*, 6099−6103.
10. Griffith, E. C., Su, Z., Turk, B. E., Chen, S., Chang, Y.-H., Wu, Z., Biemann, K., and Liu, J. O. (1997) *Chem. Biol. 4*, 461−471.
11. Pulido-Cejudo, G., Conway, B., Proulx, P., Brown, R., and Izaguirre, C. A. (1997) *Antivir. Res. 36*, 167−177.
12. Prescott, J. M., and Wilkes, S. H. (1976) *Methods Enzymol. 45B*, 530−543.
13. Chevrier, B., Schalk, C., D'Orchymont, H., Rondeau, J.-M., Moras, D., and Tarnus, C. (1994) *Structure 2*, 283−291.
14. Prescott, J. M., Wagner, F. W., Holmquist, B., and Vallee, B. L. (1983) *Biochem. Biophys. Res. Commun. 114*, 646−652.
15. Prescott, J. M., Wagner, F. W., Holmquist, B., and Vallee, B. L. (1985) *Biochemistry 24*, 5350−5356.
16. Bayliss, M. E., and Prescott, J. M. (1986) *Biochemistry 25*, 8113−8117.
17. Bennett, B., and Holz, R. C. (1997) *J. Am. Chem. Soc. 119*, 1923−1933.
18. Beattie, R. E., Elmore, D. T., Williams, C. H., and Guthrie, D. J. S. (1987) *Biochem. J. 245*, 285−288.
19. Meinnel, T., Patiny, L., Ragusa, S., and Blanquet, S. (1999) *Biochemistry 38*, 4287−4295.
20. Bond, M. D., Holquist, B., and Vallee, B. L. (1986) *J. Inorg. Biochem. 28*, 97−105.

21. Lopreore, C., and Byers, L. D. (1998) *Arch. Biochem. Biophys. 349*, 299−303.
22. Weygand, F., Prox, A., Fessel, H. H., and Kwok, K. S. (1965) *Z. Naturforsch B*, 1169−1182.
23. Taylor, A., Sawan, S., and James, T. L. (1982) *J. Biol. Chem. 257*, 11571−11576.
24. Schalk, C., Remy, J.-M., Chevrier, B., Moras, D., and Tarnus, C. (1992) *Arch. Biochem. Biophys. 294*, 91−97.
25. Chen, G., Edwards, T., D'souza, V. M., and Holz, R. C. (1997) *Biochemistry 36*, 4278−4286.
26. Baker, J. O., Wilkes, S. H., Bayliss, M. E., and Prescott, J. M. (1983) *Biochemistry 22*, 2098−2103.
27. Tuppy, H., Wiesbauer, W., and Wintersberger, E. (1962) *Hoppe-Seyler's Z Physiol. Chem. 329*, 278−288.
28. Prescott, J. M., Wilkes, S. H., Wagner, F. W., and Wilson, K. J. (1971) *J. Biol. Chem. 246*, 1756−1764.
29. Bennett, B., and Holz, R. C. (1997) *Biochemistry 36*, 9837−9846.
30. Bennett, B., and Holz, R. C. (1998) *J. Am. Chem. Soc. 120*, 12139−12140.
31. DePaola, C., Bennett, B., Holz, R. C., Ringe, D., and Petsko, G. (1999) *Biochemistry 38*, 9048−9053.
32. Chevrier, B., D'Orchymont, H., Schalk, C., Tarnus, C., and Moras, D. (1996) *Eur. J. Biochem. 237*, 393−398.
33. Mock, W. L., Chen, J. T., and Tsang, J. W. (1981) *Biochem. Biophys. Res. Commun.* 389−396.
34. Bienvenue, D., Bennett, B., and Holz, R. C. (2000) *J. Inorg. Biochem. 78*, 43−54.
35. Huntington, K. M., Bienvenue, D., Wei, Y., Bennett, B., Holz, R. C., and Pei, D. (1999) *Biochemistry 38*, 15587−15596.

BI011752O